Orbital
The electronic journal of chemistry

the electronic journal of chemistry

Technical Note | http://dx.doi.org/10.17807/orbital.v17i3.22493

Development and Evaluation of an Electromechanical Flowmeter for Volumetric Flow Measurement: Applications in Wastewater-based Epidemiology and Microplastic Monitoring in Aquatic Environments

Carlos Eduardo Rodrigues Augusto* [a], Guilherme José de Paula Gonçalves [a], Arthur Tavares Schleicher [b], Alexandre Fonseca [a], and Fernando Fabriz Sodré* [a]

Flow measurement is essential in environmental studies, enabling the calculation of contaminant loads in water and wastewater flows and supporting impact assessments. In wastewater-based epidemiology (WBE), for example, measuring influent flow at wastewater treatment plants (WWTPs) is critical for estimating population exposure to drugs and viruses. Mechanical flow meters are also valuable for microplastic studies in aquatic environments, as they measure water volumes passing through plankton nets during sampling. To address the need for reliable and cost-effective flow data, in this study a low-cost electromechanical flowmeter was developed. The device features a compact electronic system based on an Arduino Pro Mini board, sensors, an OLED display, and other components, allowing remote monitoring of rotations, time, and battery autonomy. The structure comprises an acrylic tube, 3D-printed impeller, caps for waterproofing, and supports for electronic circuits. The device demonstrated accurate measurements, was waterproof, compact, and adaptable to various applications. It offers a cost-effective solution, approximately 50 times cheaper than market alternatives, paving the way for innovations in WBE and microplastic research.

Graphical abstract

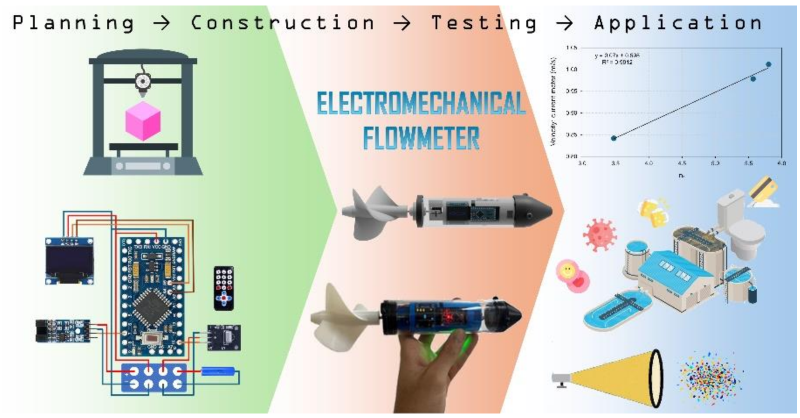

Keywords
3D printing
Instrumentation
Microplastics
Mechanical flowmeter
Wastewater-based epidemiology

Article history
Received 12 Dec 2024
Accepted 28 May 2025
Available online 30 May 2025

Handling Editor: Adilson Beatriz

1. Introduction

[a] Institute of Chemistry, University of Brasília (UnB). Campus Darcy Ribeiro - Asa Norte, zip code 70910-000, Brasília, Distrito Federal, Brazil. [b] Faculty of Technology, Department of Civil and Environmental Engineering, University of Brasília (UnB). Campus Darcy Ribeiro - Asa Norte, zip code 70910-000, Brasília, Distrito Federal, Brazil. *Corresponding author. E-mail: **ffsodre@unb.br**

Flow measurement plays a central role in various environmentally relevant studies, serving as an essential component in water resource management. This type of measurement is applied in diverse areas, such as water supply, environmental monitoring, pollution control, wastewater treatment, among others [1–3].

Monitoring the flow of rivers and reservoirs allows for the prediction of extreme weather events, such as floods and droughts, while also supporting the planning of water use for various purposes, including human consumption and irrigation. Regarding water quality, measuring volumetric flow is essential for calculating the pollutant load entering and being transported within a water body. The United States Environmental Protection Agency (EPA) recommends the development of Total Maximum Daily Loads (TMDLs) for various pollutants and water bodies [4]. This strategy is crucial to ensure that a waterbody meets and continues to meet water quality standards for specific pollutants and has inspired studies on water quality control in the United States [5,6] and in various countries, such as South Korea [7], China [8,9], Malaysia [10], and Brazil [11].

In wastewater treatment plants (WWTP), flow measurement is crucial, as operations must be properly scaled to ensure maximum treatment efficiency while optimizing resource use. The most used devices in WWTPs are Parshall flumes. These structures are characterized by their simple design, good measurement accuracy, and relatively low cost. However, proper installation is essential, following standards such as ASTM D1941 [12] and ISO 9826 [13].

In recent years, wastewater flow measurement has become mandatory in various epidemiological surveillance studies. During the COVID-19 pandemic, for instance, measuring wastewater flow enabled the calculation of SARS-CoV-2 viral loads in different regions worldwide, including Brazil [14]. This was essential for tracking the spread of the virus, monitoring disease outbreaks, developing early warning systems, and implementing containment measures [15]. This strategy, known as wastewater-based epidemiology (WBE), relies on the quantification of biomarkers, typically in samples collected at the influent of WWTPs [16].

Currently, WBE is being applied to estimate illicit drug consumption, identify new psychoactive substances, monitor the misuse of controlled pharmaceuticals, and assess the spread of viruses, bacteria, and other indicators related to human and environmental health [17–21]. However, wastewater flow measurement is not always performed in alignment with the specific needs of the WBE approach, where composite samples are often collected over 24-hour periods and across several consecutive days, requiring continuous flow monitoring throughout the sampling campaign [22]. Additionally, Parshall flumes are sometimes installed downstream of the treatment unit, which prevents accurate measurement of flow variations at the WWTP influent. While advanced measurement devices such as electromagnetic and ultrasonic sensors are available, their high cost often limits their adoption and widespread use.

In this context, mechanical impeller-based flowmeters represent a cost-effective and portable alternative for stationary applications, such as monitoring flows in rivers, channels, and outfalls. These devices function similarly to calibrated hydrometric current meters, where the number of impeller rotations, recorded over a specified time interval, correlates directly with flow velocity. This type of meter is portable, does not require any construction for installation, allows for continuous flow measurement or measurements at defined time intervals within a sampling period, and can be used in WWTPs that do not have flow measurement for the influent wastewater.

Mechanical flowmeters are also widely used in the study of microplastics in surface waters, where sample collection is typically achieved by towing plankton nets. These devices are installed at the entrance of the net to control the water flow passing through the sampler and estimate the total volume collected after a specified towing period [23,24].

Given the demand for reliable flow data to support two key research areas of the AQQUA Group at the University of Brasília (UnB), this study aimed to design, construct, and evaluate a low-cost mechanical flowmeter for volumetric flow measurements in wastewater channels and during plankton net operations.

2. Material and Methods

Electronic components

Given the various technologies available for constructing a compact and reliable flowmeter, an electromechanical device was chosen, where the counting of the impeller rotations was based on the construction of a compact electronic structure using an Arduino Pro Mini board, sensors, OLED display, and other components to enable remote monitoring of the rotation count, time, and battery life. **Fig 1** shows the wiring diagram used for the electronic system, highlighting the components employed.

To provide an innovative solution and simplify the fabrication process, technological components that enabled remote access and delivered more precise and clear information were chosen. The first step involved selecting the components, focusing on the need for a compact and autonomous structure. The Arduino Pro Mini board was selected for its low power consumption, which allowed the collection and availability of data such as the number of rotations of the impeller, battery level, and system reset status for long-term use.

To display all information accurately and in real time, a 128x64 pixel OLED display with SSD1306 controller (**Fig 1A**) was integrated into the system, exhibiting data processed by the Arduino board (**Fig 1C**). The number of rotations was measured using an infrared optical encoder speed sensor (**Fig 1B**), based on LM393 IC, which generated a signal interruption with each complete rotation. The entire system was powered by a 4.2 V 18650 lithium rechargeable battery (**Fig 1E**), which ensured the necessary autonomy for continuous operation. A battery charging module (**Fig 1F**) was also included.

The programming code was developed in C++ using the Arduino IDE. Initially, the focus was on counting the number of rotations, where each signal interruption at the optical switch of the encoder speed sensor represented a complete turn, corresponding to one rotation of the impeller. For sending user commands to the flowmeter, a remote control with an infrared transmitter/receiver (**Fig 1D**), based on the AX-1838HS IC, was used. Instructions were added to display the number of rotations and sampling time, along with battery level on the OLED screen. Only two buttons on the remote control were used. The "0" button reset the system, clearing the time count and the number of rotations, while the "OK" button displayed the data on the OLED screen. The programming was developed to automatically start counting both time and rotations as soon as the first rotation is detected, with the flowmeter already submerged.

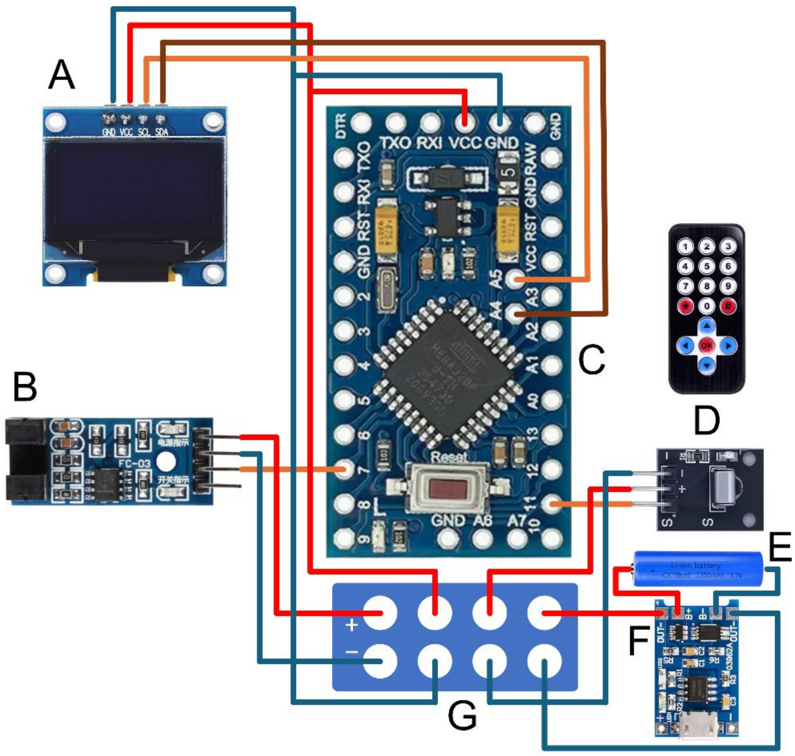

Fig. 1. Wiring diagram of electronic components (not to scale) used in the internal assembly of the flowmeter: (A) OLED display module, (B) speed encoder sensor module, (C) Arduino Pro Mini board, (D) infrared sensor and remote control, (E) rechargeable lithium battery, (F) battery charging module, and (G) power distribution bus bar.

Structure Fabrication and Assembly

Mechanical flowmeters require a compact, waterproof, and optimized structure compatible with fluid dynamics. Based on these requirements, specific details were defined to ensure functionality and the compatibility of the external components with the internal structure. **Fig 2** shows a 3D exploded view of the proposed flowmeter.

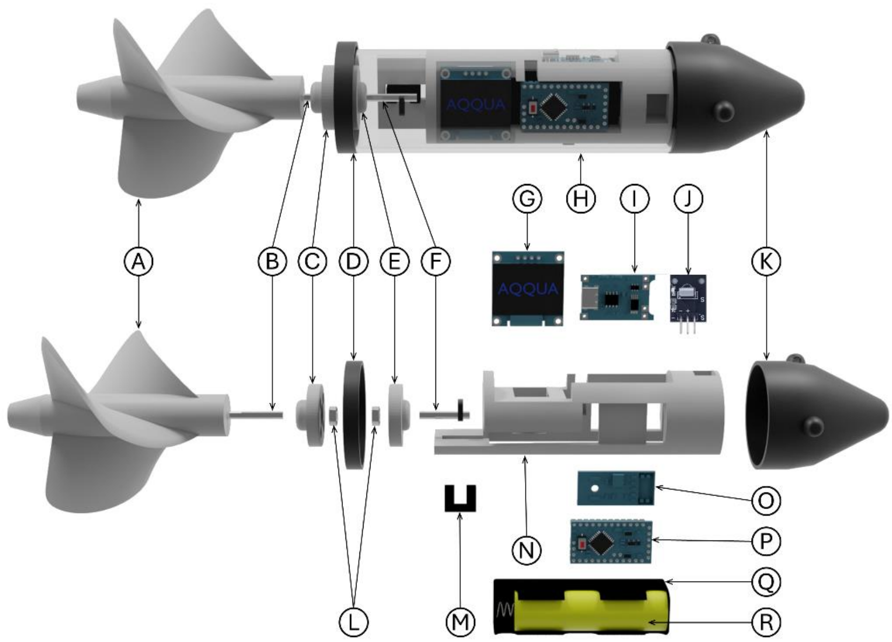

Fig. 2. Exploded-view schematic illustration of the electromechanical flowmeter designed in this work. A: impeller, B: stainless steel shaft, C: outer bearing/magnets support, D: rear cap, E: inner bearing/magnets support, F: inner steel shaft with an offset pointer, G: OLED display module, H: acrylic tube, I: battery charging module, J: infrared sensor, K: nose cone cap, L: double shielded steel ball bearings, M: optical switch of the encoder speed sensor, N: structure for integrating electronic modules, O: encoder speed sensor module, P: Arduino Pro Mini board, Q: battery holder, R: rechargeable lithium battery.

An acrylic tube (140 mm in length, 40 mm outer diameter, 36 mm inner diameter) was selected as the outer structural element of the flowmeter, as it minimizes the overall weight while preserving visibility of internal components. This transparency allows the transmission of infrared light and provides a clear view of the OLED display. Regarding other components of the flowmeter, notably items A, C, D, E, K, and N of **Fig 2**, the design was created using the 3D modeling software Blender®. All parts were 3D-printed using a Creality K1 Max 3D printer with different polymer filaments.

The three-blade impeller (**Fig 2A**) was 3D-printed in PET-G (polyethylene terephthalate glycol-modified), a mechanically strong and water-resistant material, and mounted on a 3-mm diameter stainless steel shaft (**Fig 2B**). The other end of the shaft was fitted into a PET-G support (**Fig 2C**) containing a bearing (**Fig 2L**). This support, together with the rear cover (**Fig 2D**) and a similar support installed inside the flowmeter (**Fig 2E**), forms a system designed to enable smooth impeller rotation while preventing water from entering the internal system.

The rear cap, 3D-printed with PET-G, was designed to house both the outer and inner bearing supports. In each support, four neodymium magnets were fixed equidistantly with opposing polarities between the inner and outer parts, creating synchronized movement through magnetic force. This magnetic system enables proper interaction between the two parts, while keeping water outside the acrylic tube and ensuring precise rotation of the impeller. Details of this neodymium magnet system are shown in **Fig 3**.

At the inner bearing/magnets support, another 3-mm diameter steel shaft was attached with an offset pointer at its end (**Fig 2F**). As the impeller rotates, this offset pointer interrupts the signal of the optical switch (**Fig 2M**) in the speed sensor, generating one count for each complete rotation. To enable this function, the optical switch was detached from the encoder speed sensor (**Fig 2O**) and reinstalled near the pointer.

To support the electronic modules displayed in **Fig 1**, a single-piece structure (**Fig 2N**) was designed considering the arrangement of connections, optimized performance, efficient compactness, and access points for electronic parts, while also allowing external visibility of the internal components. This structure was 3D-printed using PLA, a lightweight and durable material.

A nose cone cap (**Fig 2K**) was designed to ensure fluid dynamics and 3D-printed with PET-G. Small lead spheres were added inside this cap to increase the flowmeter front weight, promoting greater stability when submerged. Additionally, the nose cone cap features three small holders designed to attach the flowmeter to plankton nets, commonly used during microplastic collection. **Fig 4** shows the dimensions of key components of the flowmeter designed in this work. An animated video featuring several flowmeter components is also available elsewhere [25].

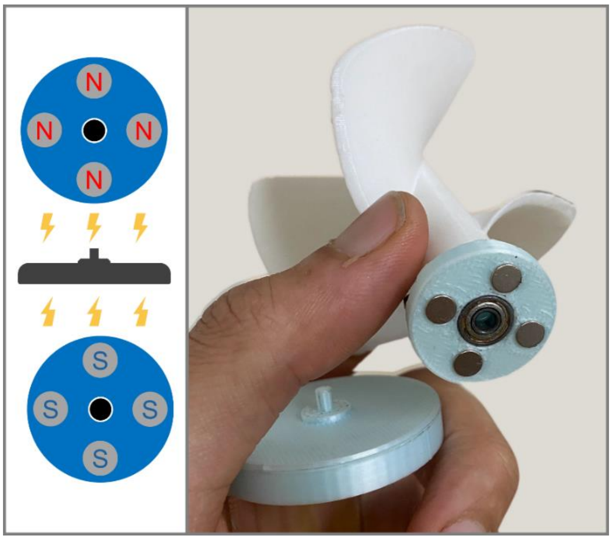

Fig. 3. Schematics and photograph of the neodymium magnet system used in the flowmeter.

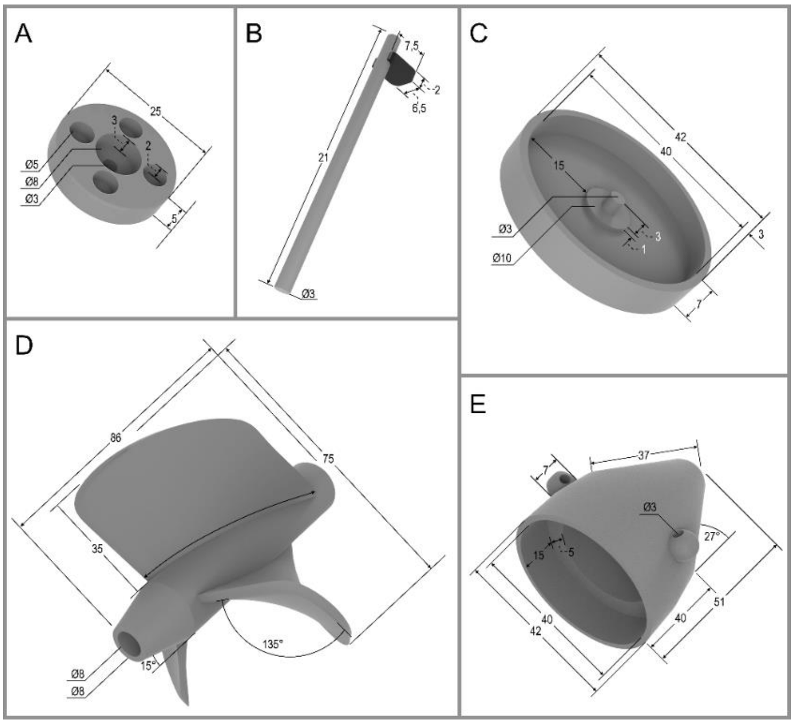

Fig. 3. Components of the flowmeter and their dimensions. A: bearing/magnets supports, B: inner steel shaft with an offset pointer, C: rear cap, D: three-blade impeller, and E: nose cone cap.

Calibration and Testing

After completing the equipment structure, an evaluation of the applicability of the system was performed. To achieve this, situations of flowmeter use in sampling contexts were simulated. The device was tested in a 15-meter-long, 300-mm-width, rectangular cross section hydraulic flume with variable slope, allowing the evaluation at different flow velocities, thus simulating typical WWTP flow rates. During the tests, water depth was adjusted by changing the bottom slope and adjusting the opening of an upstream sluice gate to enable higher water velocities.

For calibration and system evaluation, an OTT universal current meter was used coupled with an OTT Hydrometrie Z30 rotation counter. This device measures flow velocity in meters per second (m/s) at a specific point in a cross section. For all measurements, the current meter positioned at the center of the cross-section width and set at a height equal to 40% of the water depth from the flume bottom.

The velocity obtained using the current meter was then compared with the velocity monitored by the proposed electromechanical flowmeter. The bed velocity (v) was calculated using Equation 1, applicable when the number of rotations per second of the current meter (n_{cm}) exceeds 6.45 (R/t). This allowed the determination of the reference velocity, which was then compared to the number of rotations recorded by the proposed flowmeter (n_f).

$$v = 0{,}0545(R/t) + 0{,}049 \quad (1)$$

3. Results and Discussion

Fig 4 presents images of the electromechanical flowmeter developed in this work. Multiple prototypes were designed and tested, providing a range of results and insights that guided new attempts. These results were essential for obtaining the final prototype, as each iteration underscored the need for adjustments, both in the electronic system and the physical structure.

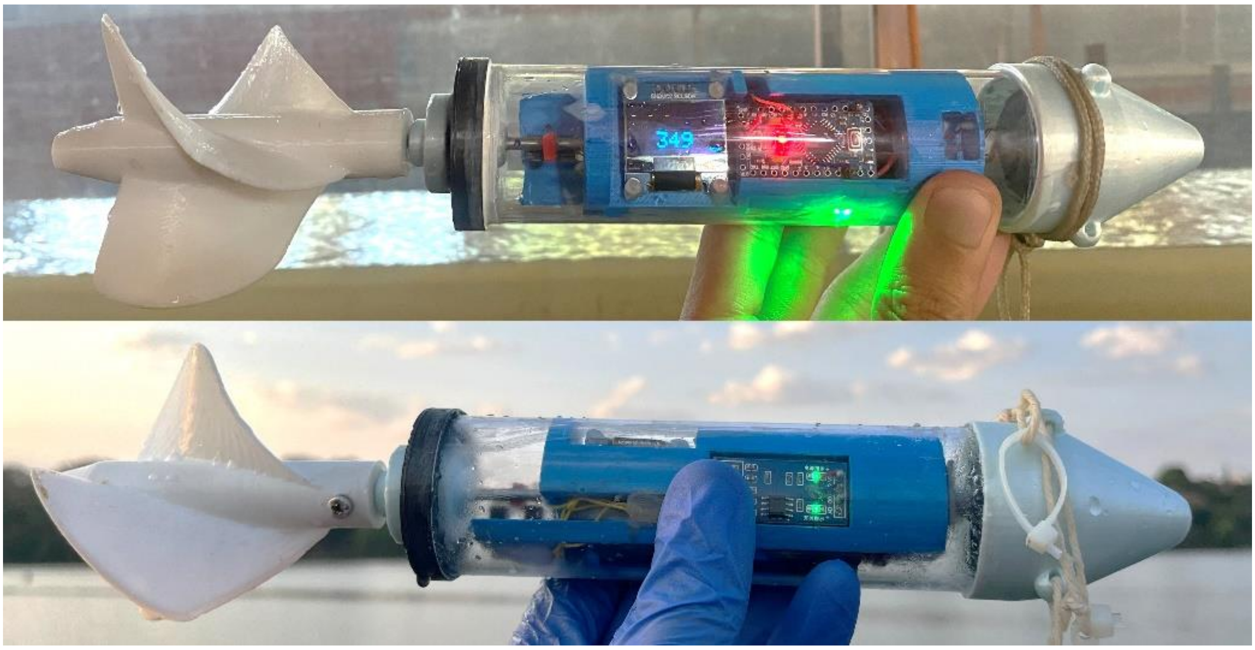

Fig. 4. Photographs of the electromechanical flowmeter developed in this work.

Electronic System

The proposed electronic setup met the expected performance. The remote control, despite operating with simple commands, responded accurately and immediately, whether submerged or not, during the applicability tests.

Compared to analog flowmeters, the addition of a time measurement on the display was an important improvement, as the sampling period count is crucial for data collection and subsequent calculations. Furthermore, the system proved effective in reading and transmitting the velocity sensor signals, with the values correctly displayed on the OLED screen. Although the system functioned adequately with the lithium battery, providing eight hours of continuous operation, the recharging process was hindered due to the complete sealing of the system, leaving no external access to the charging port.

External Structure and Sealing

One of the main challenges of the project was waterproofing the electronic components. Numerous tests were conducted to assess the sealing of different materials and components, such as shafts, bearings, and charging ports. Among the filaments tested, PLA, TPU, and PET-G showed good sealing performance. However, occasional flaws in 3D-printing resolution caused small cracks, which affected, in some cases, the impermeability.

Preliminary tests showed that incorporating a single shaft in the rear cap, along with a charging port, resulted in water intrusion, demonstrating that these alternatives were not suitable. Switching to a neodymium magnets system for impeller rotation proved more efficient, effectively eliminating a direct pathway for water entry.

During the tests, it was necessary to add weight to the front part of the flowmeter, which was achieved by placing lead spheres inside the nose cone cap. This increased ballast and submersion, as the low front weight had compromised measurement accuracy at low speeds due to higher buoyancy than drag.

Other components, such as the impeller, shaft, and bearings, performed excellently, ensuring smooth movement. Also noteworthy were the 3D-printed holders on the nose cone cap, which were essential for stabilizing the flowmeter during the calibration process. The external structure demonstrated excellent hydrodynamic characteristics, with performance comparable to other commercial measurement devices previously used and tested in the same 15-meter-long hydraulic flume.

Calibration and Use of the Flowmeter

The electromechanical flowmeter was tested at five different slopes of the hydraulic flume to assess its performance under varying flow rates. The measurements were taken in duplicate, beginning with the flowmeter and followed by the reference current meter. **Table 1** presents the data obtained during this calibration process.

Table 1. Measurements for bed velocity calculation using the flowmeter and the reference current meter.

Measurement	Water Depth (mm)	Time (s)	Flowmeter rotations	Current meter rotations (R)
1	75.1	60	367	1381
			364	1387
2	83.2	60	353	1098
			352	1080
3	92.1	60	367	1064
			364	1056
4	100.3	60	333	1023
			335	1024
5	119.6	60	224	875
			193	871

Based on Equation 1, it was possible to calculate the flow velocity, since the number of rotations of the current meter (n_{cm}) was significantly greater than 6.45 for all measurements. **Table 2** shows the average velocity obtained by the current meter, as well as the average number of rotations recorded by both the current meter and the electromechanical flowmeter.

In **Fig 5**, only three points were used to construct the calibration curve, aiming for a higher determination coefficient (R^2). However, despite an R^2 of 0.9912, this value was deemed satisfactory. Additionally, a deviation from linearity was observed for bed velocities greater than approximately 1.0 m/s, which requires further calibration steps, which will involve using a rod to provide greater steadiness to the flowmeter during the tests.

Table 2. Calculated values for n_{cm} and n_f, and for the reference current meter velocity.

Measurement	n_f	n_{cm}	Average velocity (m/s)
1	6.0917	23.067	1.3061
2	5.8750	18.150	1.0382
3	5.8000	17.667	1.0118
4	5.5667	17.058	0.9787
5	3.4750	14.550	0.8420

During measurement #5, although the impeller could rotate, the rotation did not occur continuously due to the low drag force resulting from the reduced flow/velocity. This explains the discrepancy between the replicates of this measurement, as shown in **Table 1**. Based on the data obtained for the average velocity and the number of rotations recorded by the flowmeter, it was possible to create the calibration curve presented in **Fig 5**.

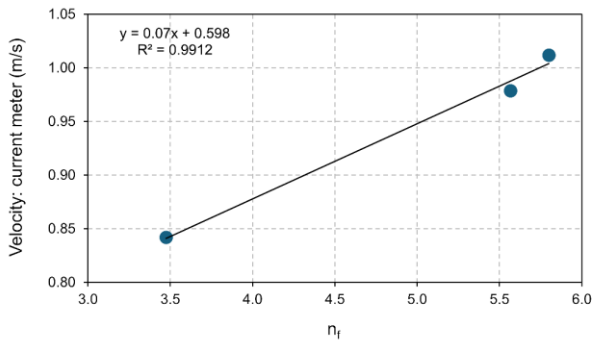

Fig. 5. Calibration curve for the electromechanical flowmeter developed in this work.

Cost Evaluation

The cost of the materials used was a key parameter in the design and construction of the device. **Table 3** presents the evaluation of the prices of each material used in the construction of the electromechanical flowmeter unit.

Table 3. Materials used for the construction of the electromechanical flowmeter developed in this work

Item	Description	Quantity	Unit Price (US$)*
1	Filament FLEX TPU 98A Black	20 g	0.56
2	Filament Creality CR-PETG	20 g	0.54
3	Filament PLA	20 g	0.37
4	Acrylic Tube Ø40 mm	15 cm	3.58
5	Arduino Pro Mini 328 5 V / 16 MHz	1 unit	5.33
6	Lithium Battery 4.2 V 18650	1 unit	2.35
7	Lithium Battery Holder 18650	1 unit	0.68
8	Speed Sensor Encoder Module	1 unit	1.04
9	OLED Display 128x64 0.96"	1 unit	6.30
10	Stainless Steel Rod 3 x 500 mm	1 unit	1.92
11	Neodymium Magnet 3 x 1.5 mm	8 unit	0.27
12	IR Remote Control Kit	1 unit	2.32
13	Sikaflex-291i Sealant and Adhesive	1/5 unit	2.42
14	Lead Fishing Balls	100 g	0.10
		TOTAL	27.78

*Considering the values practiced in the Brazilian market and converted to US$.

The listed items are presented with their prices and unit quantities, sufficient to assemble a single prototype of the flowmeter, assuming 3D printers are already available. Additionally, three different types of filaments were used throughout the prototype development process to evaluate the adaptability of each, although only one type was necessary for the operation of the device. Despite using multiple materials, the final value of approximately US$ 30.00 still represents a significant saving (up to 50 times), considering that similar commercial devices can cost between US$ 1,000.00 and US$ 1,500.00 in Brazilian retail.

4. Conclusions

This work resulted in the development of an electromechanical flowmeter designed to support studies on wastewater-based epidemiology and microplastic sampling in surface waters. Several challenges were overcome during the design of the device, particularly in terms of the electronic system and physical structure, leading to the creation of different prototypes and significant improvements throughout the project.

The electronic system performed as planned, with a responsive remote control and accurate measurements, although accessing the battery for recharging posed a challenge due to the sealed design of the unit. Waterproofing was prioritized, and the choice of appropriate filaments ensured protection, despite occasional failures.

Calibration of the flowmeter at different speeds demonstrated the effectiveness of the device, but also highlighted areas for improvement, particularly for velocities exceeding 1.0 m/s. Adding weight to the front ensured stability during measurements.

Cost analysis revealed that the developed flowmeter could be 50 times cheaper than similar devices available on the Brazilian market, highlighting its economic attractiveness.

Future improvements should focus on reassessing battery charging access, improving submersion at varying speeds (especially at low velocities), exploring techniques to increase waterproofing, and conducting *in situ* wastewater flow measurements. This work not only met the proposed objectives but also paved the way for innovations that enable the execution of diverse related research projects.

Acknowledgments

CERA thanks Foundation for Research Support of the Federal District (FAPDF) and the Scientific Initiation Program of the University of Brasília (PIBIC) for the scholarship. FFS thank National Council for Scientific and Technological Development (CNPq) for fellowship (Grant 314341/2020−0). This study was funded by the National Institute of Advanced Analytical Science and Technology (INCTAA), under Grant CNPq 465768/2014-8, and the Ministry of Justice and Public Security, under Grant TED/UnB/SENAD 04/2020.

Author Contributions

Carlos E. R. Augusto: Data curation, Formal analysis, Investigation, Methodology, Validation, Writing - Original Draft. Guilherme J. P. Gonçalves: Data curation, Formal analysis, Methodology, Software, Validation. Arthur T. Schleicher: Data curation, Formal analysis, Methodology, Validation, Visualization, Writing - Review & Editing. Alexandre Fonseca: Conceptualization, Data curation, Formal analysis, Methodology, Software, Supervision, Validation, Visualization, Writing - Review & Editing. Fernando F. Sodré: Conceptualization, Data curation, Funding acquisition, Project administration, Supervision, Visualization, Writing - Original Draft, Review & Editing.

References and Notes

[1] Luo, M.; Liu, X.; Legesse, N.; Liu, Y.; Wu, S.; Han, F.X.; Ma, Y. *Water, Air, Soil Pollut*. **2023**, *234*, 657. **[Crossref]**

[2] Hashemi Monfared, S.A.; Dehghani Darmian, M.; Snyder, S.A.; Azizyan, G.; Pirzadeh, B.; Azhdary Moghaddam, M. *Bull. Environ. Contam. Toxicol.* **2017**, *99*, 531. **[Crossref]**

[3] Fleming, P. M.; Stephenson, K.; Collick, A.S.; Easton, Z.M. *J. Environ. Manage.* **2022**, *308*, 114649. **[Crossref]**

[4] Available from: **https://www.epa.gov/tmdl/overview-total-maximum-daily-loads-tmdls.** Access December, 2024.

[5] Chen, C. W.; Herr, J.; Ziemelis, L.; Goldstein, R. A.; Olmsted, L. *J. Environ. Eng.* **1999**, *125*, 653. **[Crossref]**

[6] Borah, D. K.; Zhang, H. X.; Zellner, M.; Ahmadisharaf, E.; Babbar-Sebens, M.; Quinn, N. W. T.; Kumar, S.; Sridharan, V. K.; Leelaruban, N.; Lott, C. *J. Environ. Eng.* **2024**, *150*, 3124003. **[Crossref]**

[7] Kwon, H.; Jo, C.; Choi, S. *Environ. Technol. Innov.* **2023**, *32*, 103251. **[Crossref]**

[8] Wang, Z.; Zou, R.; Zhu, X.; He, B.; Yuan, G.; Zhao, L.; Liu, Y. *Int. J. Environ. Sci. Technol.* 2014, *11*, 423. **[Crossref]**

[9] Wang, C.; Bi, J.; Ambrose, R. B. *Ecol. Eng.* **2015**, *83*, 258. **[Crossref]**

[10] Adnan, M. S.; Roslen, H.; Samsuri, S. *IOP Conf. Ser. Earth Environ. Sci.* **2022**, *1022*, 12074. **[Crossref]**

[11] da Silva, G. S.; Jardim, W. F. *Quim. Nova* **2007**, *12*, 160. **[Crossref]**

[12] American Society for Testing and Materials, ASTM D1941-21: Standard Test Method for Open Channel Flow Measurement of Water with the Parshall Flume, 2021.

[13] International Organization for Standardization, ISO 9826:1992: Measurement of Liquid Flow in Open Channels - Parshall and SANIIRI Flumes, 2023.

[14] Bueno, R. F.; Claro, I. C. M.; Augusto, M. R.; Duran, A. F. A.; Camillo, L. M. B.; Cabral, A. D.; Sodré, F. F.; Brandão, C. C. S.; Vizzotto, C. S.; Silveira, R.; Mendes, G. M.; Arruda, A. F.; de Brito, N. N.; Machado, B. A. S.; Duarte, G. R. M.; Aguiar-Oliveira, M. L. *J. Environ. Chem. Eng.* **2022**, *10*, 108298. **[Crossref]**

[15] Sodré, F. F.; Brandão, C. C. S.; Vizzotto, C. S.; Maldaner, A. O. *Quim. Nova* **2020**, *43*, 515. **[Crossref]**

[16] Lorenzo, M.; Picó, Y. *Curr. Opin. Environ. Sci. Heal.* **2019**, *9*, 77. **[Crossref]**

[17] Bade, R.; Rousis, N.; Adhikari, S.; Baduel, C.; Bijlsma, L.; Bizani, E.; Boogaerts, T.; Burgard, D. A.; Castiglioni, S.; Chappell, A.; Covaci, A.; Driver, E. M.; Sodre, F. F.; Fatta-Kassinos, D.; Galani, A.; Gerber, C.; Gracia-Lor, E.; Gracia-Marín, E.; Halden, R. U.; Heath, E.; Hernandez, F.; Jaunay, E.; Lai, F. Y.; Lee, H.-J.; Laimou-Geraniou, M.; Oh, J.-E.; Olafsdottir, K.; Phung, K.; Castro, M. P.; Psichoudaki, M.; Shao, X.; Salgueiro-Gonzalez, N.; Feitosa, R. S.; Gomes, C. S.; Subedi, B.; Löve, A. S. C.;

Thomaidis, N.; Tran, D.; van Nuijs, A.; Verovšek, T.; Wang, D.; White, J. M.; Yargeau, V.; Zuccato, E.; Mueller, J. F. *Water Res. X* **2023**, *19*, 100179. **[Crossref]**

[18] Bade, R.; van Herwerden, D.; Rousis, N.; Adhikari, S.; Allen, D.; Baduel, C.; Bijlsma, L.; Boogaerts, T.; Burgard, D.; Chappell, A.; Driver, E. M.; Sodre, F. F.; Fatta-Kassinos, D.; Gracia-Lor, E.; Gracia-Marín, E.; Halden, R. U.; Heath, E.; Jaunay, E.; Krotulski, A.; Lai, F. Y.; Löve, A. S. C.; O'Brien, J. W.; Oh, J.-E.; Pasin, D.; Castro, M. P.; Psichoudaki, M.; Salgueiro-Gonzalez, N.; Gomes, C. S.; Subedi, B.; Thomas, K. V; Thomaidis, N.; Wang, D.; Yargeau, V.; Samanipour, S.; Mueller, J. *J. Hazard. Mater.* **2024**, *469*, 133955. **[Crossref]**

[19] Gomes, C. S.; Freire, D. J. S.; Moura, H. S. R. P.; Maldaner, A. O.; Pinheiro, F. A. S. D.; Ferreira, G. L. R.; Miranda, M. L. O.; Ferreira, L. D. S.; Murga, F. G.; Sodré, F. F.; Aragão, C. F. S. *Drug Test. Anal.* **2024**, Early View. **[Crossref]**

[20] Sodré, F. F.; Freire, D. J. S.; Alcântara, D. B.; Maldaner, A. O. *Front. Anal. Sci.* **2022**, *2*, 930480. **[Crossref]**

[21] Claro, I. C. M.; Cabral, A. D.; Augusto, M. R.; Duran, A. F. A.; Graciosa, M. C. P.; Fonseca, F. L. A.; Speranca, M. A.; Bueno, R. F. *Water Res.* **2021**, *203*, 117534. **[Crossref]**

[22] de Oliveira, A. F. B.; de Melo Vieira, A.; Santos, J. M. *Anal. Bioanal. Chem.* **2023**, *415*, 3749. **[Crossref]**

[23] Gupta, D. K.; Choudhary, D.; Vishwakarma, A.; Mudgal, M.; Srivastava, A. K.; Singh, A. *Int. J. Environ. Sci. Technol.* **2023**, *20*, 6865. **[Crossref]**

[24] Stock, F.; Kochleus, C.; Bänsch-Baltruschat, B.; Brennholt, N.; Reifferscheid, G. *TrAC Trends Anal. Chem.* **2019**, *113*, 84. **[Crossref]**

[25] Available from: **https://youtu.be/3Rqi19AnxuY.** Access December, 2024.

How to cite this article

Augusto, C. E. R.; Gonçalves, G. J. P.; Schleicher, A. T.; Fonseca, A.; Sodré, F. F. *Orbital: Electronic J. Chem*. **2025**, *17*, 289. DOI: **http://dx.doi.org/10.17807/orbital.v17i3.22493**